ICESP XIII, September 2013, Bangalore, India

Electrical parameters of an operating industrial electrostatic precipitator under intermittent energization: simulation and continuous measurement analysis

Véronique ARRONDEL[1], Gianluca BACCHIEGA[2], Michel HAMLIL[1]

[1] EDF R&D, Chatou, France – veronique.arrondel@edf.fr

[2]I.R.S. s.r.l. Padova – ITALY – bacchiega@irsweb.it

Abstract:

The control systems of the electrical power supplies installed on coal power plants' electrostatic precipitators (ESP) vary. However, their basic principle of operation is the same: the aim is to maintain the maximum current (or infrequently the maximum voltage) with a limited number of sparks and no spark-over.

This mode of control, by the number of sparks per minute (adjustable per field), is not suitable in the case of back-corona. If the ash resistivity is high, then intermittent energization has to be used.
The simulation of performances of a dust collector operating under DC voltage is described extensively in the literature. This paper presents a simulation of the performances of an electrostatic precipitator powered by intermittent energization using physical models. For this reason, an equivalent electrical circuit of the electrostatic field is given, and the current-voltage characteristics are compared to those observed on an industrial site. Intermittent energization performances are then compared to those of a normal control mode.

Finally, data recorded on the dust collector of a coal-burning 250 MW unit using intermittent energization are analysed in order to detect process modification and faults in the electrostatic precipitator. This is carried out without having to stop the installation and without manual readings. Voltage current characteristics can be deduced from standard data collected continuously, thereby avoiding a specific system for acquiring data.

1. Introduction

The electrical parameters are the key factors in the performance of an electrostatic precipitator. The technology and the equipment used for the electrical power supply give different voltage forms [1], [2], [3]:

1- Traditional direct current energization, obtained by full wave rectification from 50 Hz which creates residual ripple at 100 Hz with a value between 30 % and 60 %; reducing its efficiency;

2 – Short pulsating energization, which consists of superimposing pulses from 1 µs to 100 µs on a direct current voltage, favorable to the elimination of back-corona;

3 – Low ripple rate direct current energization obtained from a high frequency system (Switched-mode power supply using 10 kHz to 50 kHz switching) which makes it possible to generate a voltage with a very low level of ripple (a few %) after rectification, therefore avoiding efficiency losses.

The control systems for the electrical power supplies installed on coal power plants vary. However, their basic principle of operation is the same: the objective is to achieve maximum performance by raising the voltage or, more often, the current, with a limited number of sparks or no spark-over [4].

This mode of control by the number of sparks per minute (adjustable per field) is not suitable in the case of energy-saving mode or when back-corona is present [5]. If the ash resistivity is high, then intermittent energization has to be used [6], [7], [8], [9], [10].

Intermittent energization is supplied by the same electrical equipment as in traditional high voltage power supplies. The difference resides in the suppression of a certain number of half-cycles of the current. So the voltage decreases which can reduce or stop back-corona discharge in the dust layer [11], [12], [13].

2. Intermittent energization simulation using a physical model

The simulation of the performances of a dust collector operating under DC voltage is described extensively in the literature. The object of this paragraph is first of all to describe how to:

- simulate the form of the voltage from the current using a simplified equivalent circuit
- estimate collection efficiency for each particle size class.

The first step deals with the definition and validation of the equivalent circuit to convert the suppression of half cycle current into a voltage waveform.

The second step focuses on the ESP performance simulation results when the degree of intermittence is 1:3 or 1:5. A physical model and the actual applied voltage waveform are used.

2.1. Intermittent voltage waveform computation using an electrical discharge current simulation and an ESP field equivalent capacity

A physical simulation of an electrostatic precipitator can be made from the voltage waveform applied to the electrodes. From these values the corona discharge current at the heart of the capture process, with or without intermittent energization, may be calculated.

The following procedure was used to define how voltage waveform can be computed:

- A simplified electrical equivalent circuit of an electrostatic precipitator is defined,
- An estimation of the field's capacity is made using ESP geometry, voltage and current measurements,
- The equivalent circuit is validated with measurements and then used to simulate the half cycle suppression.

Equivalent electric circuit

Figure 1 shows an electrostatic precipitator equivalent electrical circuit where the equivalent field capacity and electrical discharge current are given for the entire wire-plate assembly.

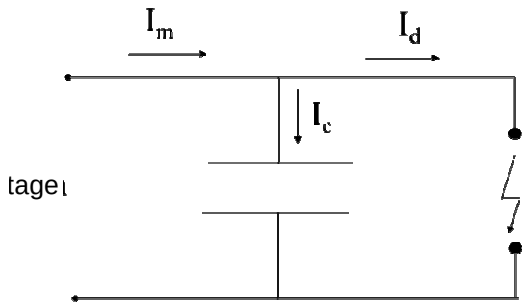

Figure 1: Simplified ESP circuit where I_m, I_c and I_d are respectively the measured, capacity and discharge current.

The discharge current directly charges the flue gas particles resulting in their capture in the filtering process and depends on the ESP geometry, on the applied voltage as well as on the quantity of the particles and on the flue gas velocity. The discharge current for a given geometry and field position can be described as a function of the voltage and the flue gas velocity as shown in the following equation:

$$I_d = (a\,V^2 + b\,V + c)\left(1 + d\,\frac{v - v_n}{v_n}\right)$$

The parameters a, b, c and d can be calculated by regression from a series of simulations [14] where the V is voltage and v is the velocity (v_n is the reference velocity value).

Estimation of a field's capacity

A first approximation can be made using geometric parameters.

Then, in order to better estimate the equivalent field capacity, the measured secondary voltage can be used. This signal is first filtered to eliminate high frequency noise, and then it is differentiated as a function of time. Accordingly, the signal obtained is directly proportional to the capacity current. Then using the approximate capacity, the discharge current can be found. In Figure 2, the capacitive and discharge currents which were estimated from recorded data are given.

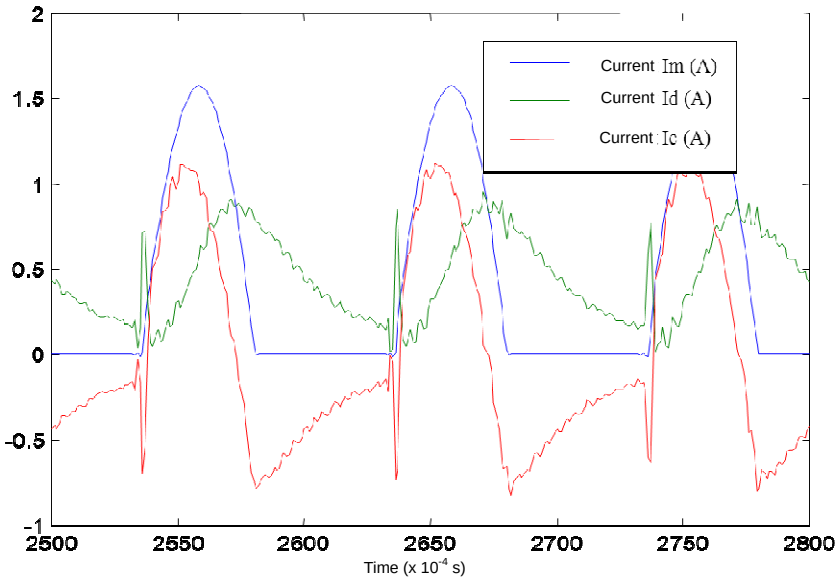

Figure 2 : Graph of the measured current (I_m in red) and currents (I_d et I_c) calculated from the measured voltage, using the equivalent circuit with an estimated capacity.

A graph of the voltage measured against the estimated discharge current allows the ESP equivalent capacity to be more precisely estimated. In fact, as the real capacity value is reached, the current and the voltage curves converge to become coincident (see Figure 4 as an example).

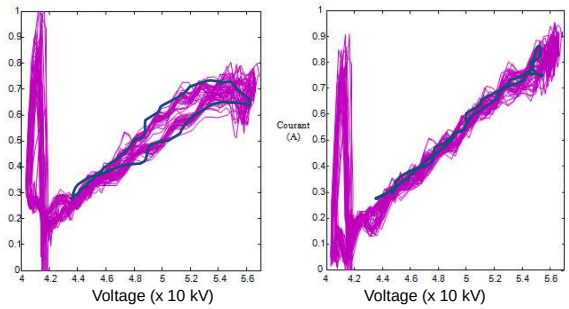

Figure 3 : Relation between the voltage and the discharge current for two capacitance values (left C_0=140. 10^{-9} Farad plot have a loop, right C_0=150. 10^{-9} Farad plot are superposed)

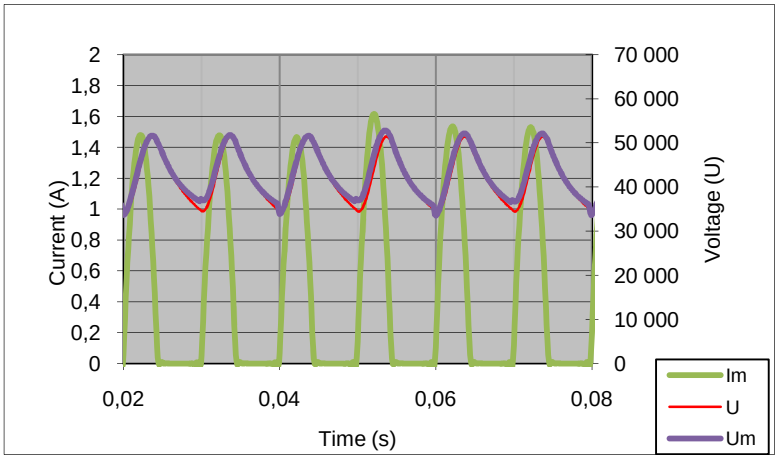

Figure 4: Comparison of simulated voltage (U) and measured voltage (U_m) ; the current of this field is I_m.

<u>Validation and estimation of discharge current with and without alternance suppressions</u>

Using the simplified electrical circuit and an applied current, the voltage and the discharge current can be calculated and compared to measurements for validation. Figure 4 compares the calculated voltage U (using the measured applied current I_m) and the experimentally measured voltage values U_m.

The parameters of the equivalent circuit can also be used to determine the discharge current for both normal and intermittent energization situations. It is assumed that the applied current pulses are identical in shape but not in frequency.

Figures 5 (standard) and 6 (half cycle current suppression) show the simulation results. The graphs show the number of applied current pulses (I) and the calculated electrical potential (V) using the equivalent circuit (Figure 1). They show that the discharge current I_d does not disappear when there is no pulse suppression, whereas it disappears when half-cycles are suppressed. Lack of discharge current means that back-corona may be extinguished.

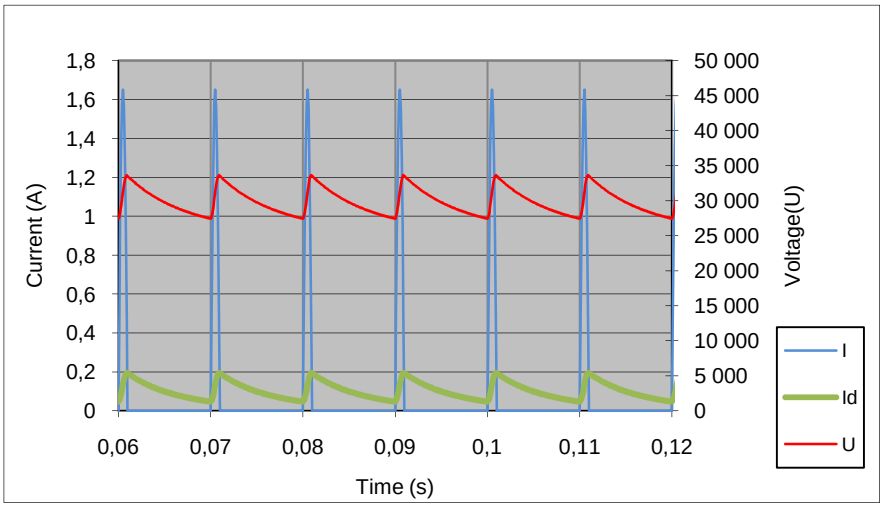

Figure 5 : Current and voltage with a current density of approx. 11 mA/m^3 without half-cycle suppression

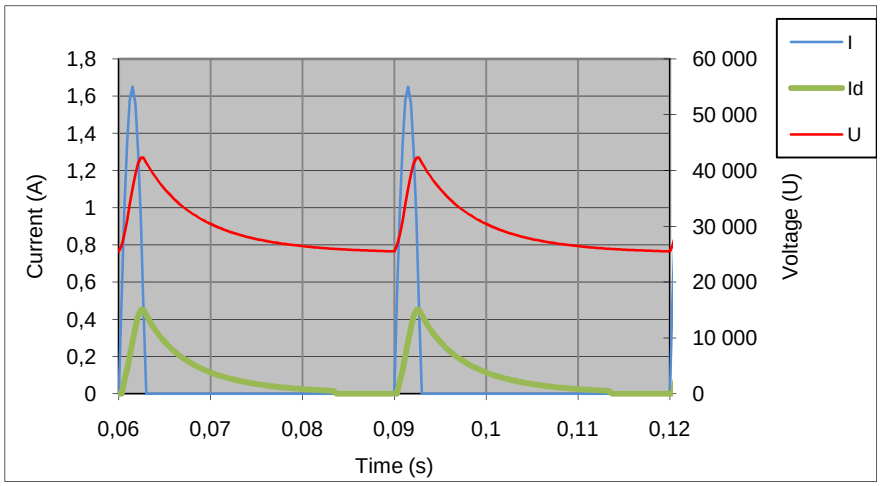

Figure 6: Current and voltage signals with 1-in-3 half-cycle suppressions

Figure 7 compares computed voltage waveforms in standard control mode (S0) with one-in-three (S3) and one-in-five (S5) half-cycle suppressions.

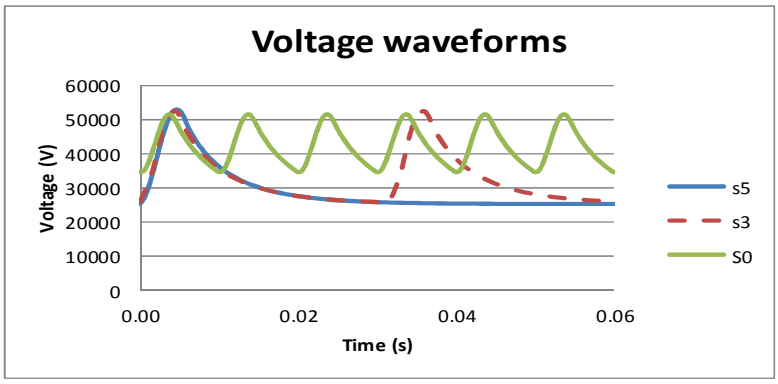

Figure 7: Comparison of standard voltage waveform (S0) with 3 and 5 half-cycles current (S3 and S5) suppression

The possibility to calculate the voltage waveforms with different numbers of current half-cycle suppressions was used to simulate the variation in the precipitator's efficiency to collect particles as a function of the number of suppressed half-cycles.

2.2. The impact of intermittent energisation on ESP efficiency simulation

From a given voltage applied to the electrodes, the ESP simulation software [15], [16], [17], [18], [19], [20], can simulate half-cycle suppressions. This software is based on physical modelling of the collection process. Using this approach, an estimation of the efficiency of the electrostatic precipitator can be made without using an experimental database. In particular, the software is able to simulate the production of ions at the wires by the corona discharge, as well as the other physical processes (gas flow modelling, particle charging, ion and particle migration).

The simulation given here focuses on one field in a precipitator. The field consists of 40 channels with a distance between the plates of 280 mm. Each channel is composed of 6 pairs of plates in series. Between each pair, positioned face to face, are two ribbons with points emitting wires. The applied voltage has one-in-five half-cycles suppressed. At the inlet of the ESP the concentration is 12 g/Nm^3 with a log-normal particle-size distribution.

A granulometric distribution into 6 classes is given in Figure 8.

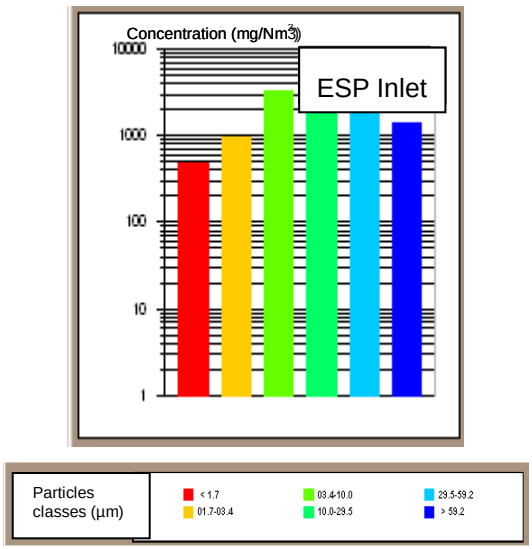

Figure 8: Granulometric log-normal distribution into 6 classes at the ESP inlet/entrance (mg/Nm^3)

Variation in flow and particle density as a function of the voltage

How do the variations in the voltage influence the particle density and the flow of dust particles ?
Figure 9 shows the two directions of flow given in Figure 10 and Figure 11. The blue arrow indicates the direction of particles collected on the plates, the red arrow indicates the direction of particles that pass out of the inter-plate zone without being collected.

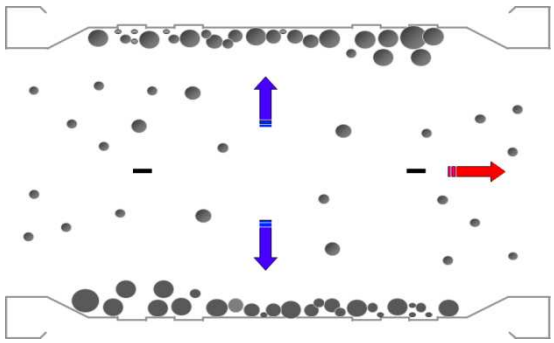

Figure 9 : Diagram showing the two studied flow rates: flow rate of particles collected by the plates (blue arrow) and flow rate of uncollected particles that come from the area bound by the plate (red arrow)

Figure 10 shows how the flow of particles onto the collecting plates changes over time. The six coloured traces correspond to the 6 plates in the simulated field.

The deposit rate on the plate varies with time. This evolution is linked to both to the voltage's periodic variation (0.06s) and to the delay time before the ESP becomes fully operational. The particle density is homogenous on entering the first inter-plate zone, as the particles enter the second and subsequent inter-plate zones the density at that entrance recopies that at the exit of the former inter-plate zone. This explains the different profile of the curve for plate 1 from those of the other plates.

The particle flow as it leaves a plate (Figure 11) does not follow the voltage variation as at this position the electric field is zero and the particles flow along in the flue gases. Figure 11 also reveals the duration of the flue gas flow (0.6s).

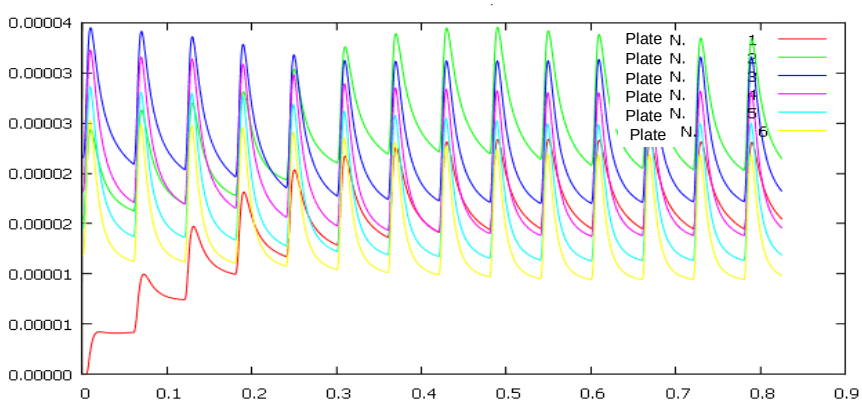

Figure 10 : Particle flow (kg/s) to the plates (from n°1 to n°6) as a function of time.

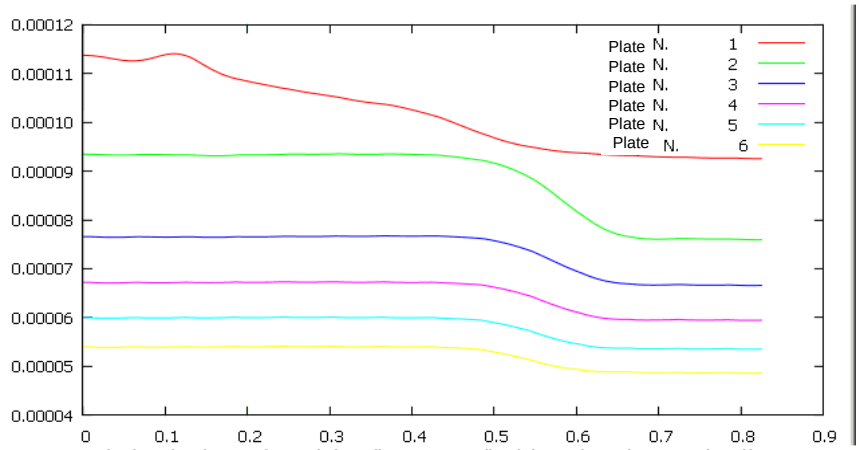

Figure 11 : Evolution in time of particles flow rates (kg/s) at the plate outlet (from n°1 to n°6).

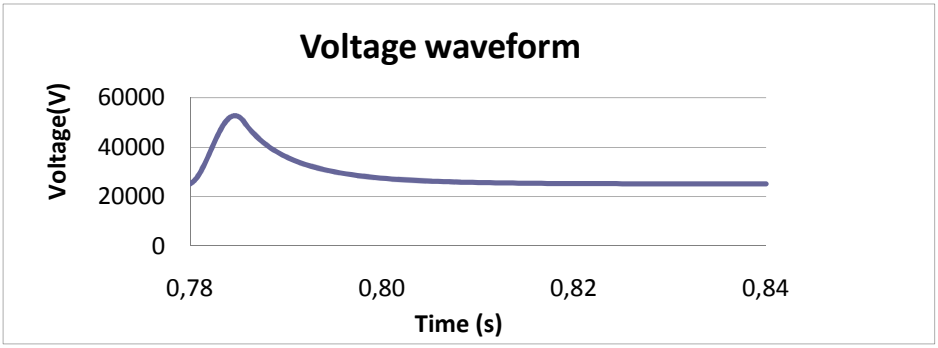

Figure 12 : Variation of the voltage over time

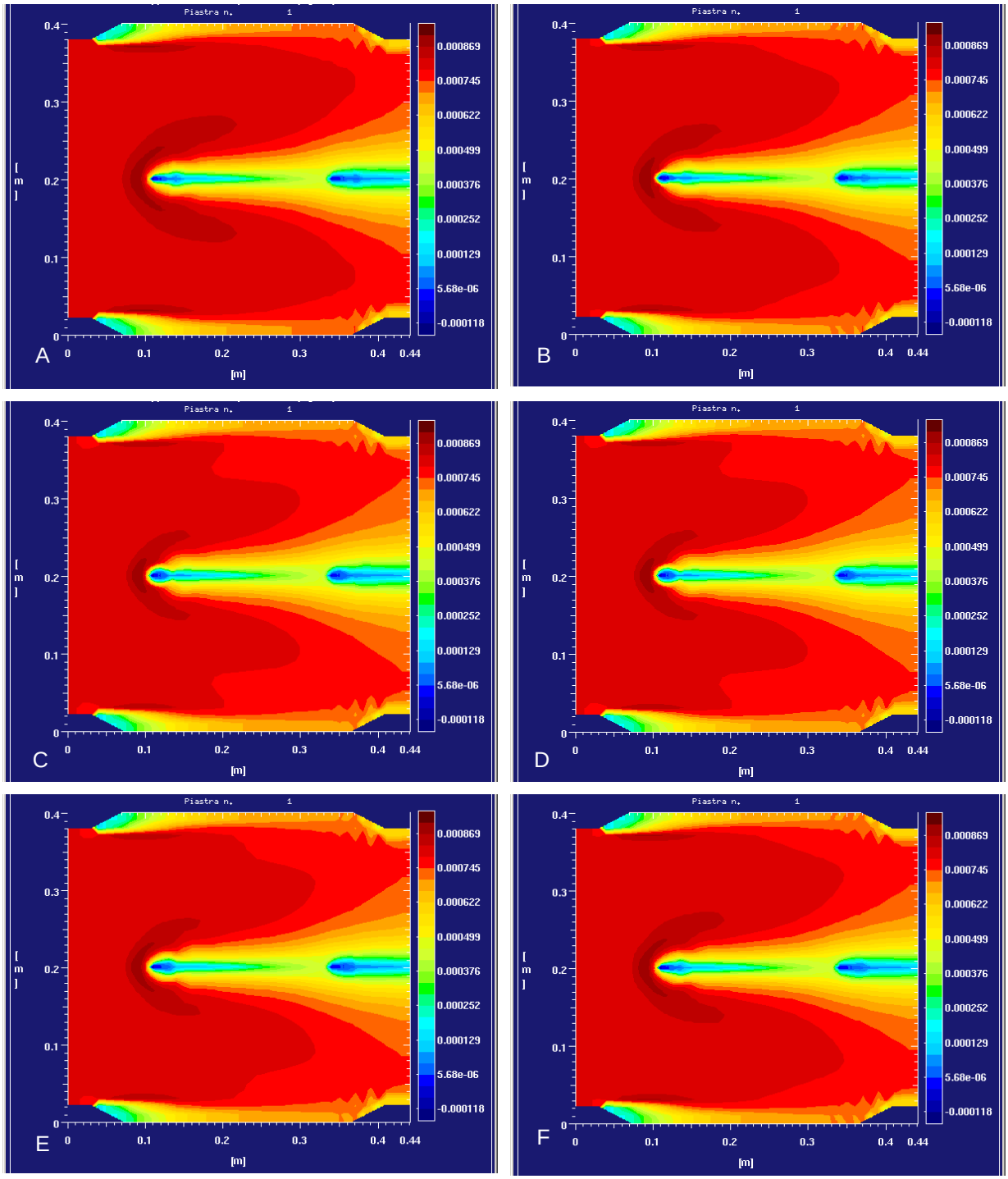

Figure 13 : Evolution of the mass concentration on plate1 at 6 different instants (A to F 0,78s, 0,79s, 0,80s, 0,81s, 0,82s and 0,83s) as a function of the voltage variation, (suppression of 5 half-cycles/one-in-five half-cycles).

The spatial concentration of the particles is represented in Figure 13 at 6 instants (every 0,01 seconds) as a function of the voltage (Figure 12). The concentration of the particles in the inter-electrode zone and so on the plates follows the voltage variation particularly well on the left electrode. At 0,78s the concentration around this electrode is high (as the voltage was low from the preceding cycle). Then the voltage increases and the particle density at the electrode falls (figures B, C and D), the particle density follows the voltage with a slight time lag. Then as the density falls, the density starts again to increase (figures E and F) as the particles migrate more slowly.

Changes in the amount of particles captured according to their granulometric class as a function of the voltage

The variation in the efficiency was studied with and without half-cycle suppression for a field in an electrostatic precipitator assuming the absence of back-corona.

The voltages defined in Figure 7 were used to simulate the particle collector operation with a DC voltage and intermittent energization, in particular with one-in-three and one-in-five half-cycle current suppressions. The simulations allowed the ESP performance results obtained from applying these types of signals to be compared.

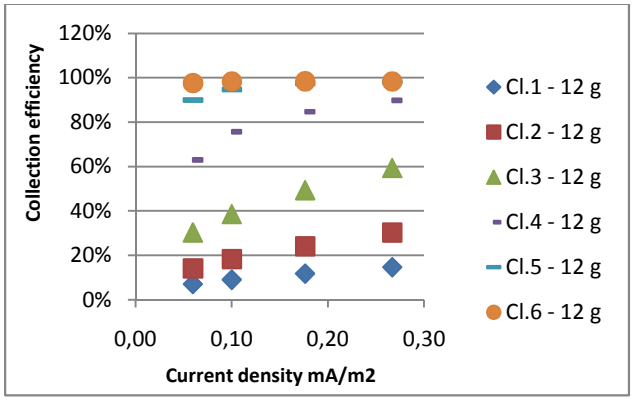

Figure 14 : The variation in the efficiency of capture of an electrofilter for 6 particle-size classes, (with half-cycle suppression), as a function of the current density, with an entry concentration of 12g/Nm^3.

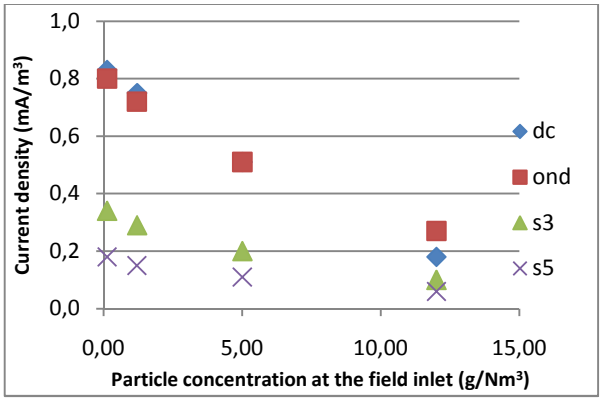

Figure 15: Variation in the current density as a function of the particle concentration at the field inlet, for a given applied voltage.

The collection efficiency for each class of particles increases with the current density. This relationship means that the collection efficiency is also linked to the half-cycle suppressions as the current density is 0,27mA/m^2 (AC or S0), with no suppression, 0,01 mA/m^2 with one-in-three half-cycle suppressions (S3) and 0.06 mA/m^2 with one-in-five half-cycle suppressions (S5). The current density is 0,18 mA/m^2 for DC energization (DC voltage equal to the mean voltage of S0).

The results of the simulation show that the efficiency for the given DC voltage is lower than for an AC but greater than when half-cycles are suppressed. In fact, the efficiency is linked to the current density which follows the same trend.

For a given applied voltage, the density of the current depends on the concentration of the particles at the inlet of the field due to the space charge (Figure 1). The AC and DC voltage curves are similar for low particle concentrations.

2.3. Conclusion

An equivalent circuit allows the shape of the voltage wave to be calculated, as a function of the applied current waveform, in order to determine the input values for the simulation of the half-cycle suppressions. It is used to check the influence of the current waveform on the ESP's performance. The simulation results for different rates of half-cycle suppression include: collection efficiency, particle concentration maps between the plates and particle flow to the plates as function of time.

3. Analysis of voltage and current parameters during intermittent energization on an operating industrial ESP

This paragraph presents the interpretation of the current-voltage data from a high-voltage power-supplied ESP in a working 250 MW industrial coal-burning, unit acquired continuously at a 1-second sampling frequency.

The data from the operating industrial ESP were analysed to reveal the following useful information:

- Current-voltages as function of time and their relationship to other parameters,
- Current-voltage measurement and their relationship to the electric unit's production,
- Current as function of voltage and the construction of the current voltage characteristics.

3.1. Current-voltages as function of time and their relation to other parameters

Variations in the current and voltage's measured can be analysed as a function of time. This on line data can be collated with other operating unit data such as: power, SO_2 level, casing's 1 and 2 inlet temperatures, particle level at the ESP outlet.

An example of the collected data is given Figure 15, where the voltage and the current are recorded for field 2. The power of this unit varies from half to full load (blue line). The level of the dust emissions is monitored by two opacimeters (one for each casing) and by a Beta probe at the chimney. The consistent quality of the coal can be checked by verifying the SO_2 concentration in the fumes. It varies between 1600 mg/Nm^3 and 2000 mg/Nm ^{3} which correspond respectively to a 0,8% and 1% sulphur content. The current (in green) and the voltage (in blue) vary with time.

This graph points out the presence of the intermittent mode (zone 1). The intermittent mode corresponds to back-corona detection by T/R control, which as expected, is concurrent with the moment of the weakest SO_2 flue gas concentration. In addition, the dust emission continues to increased.

Figure 15 also reveals a time interval where the power supply is out of service (the current is zero around 10:00) (zone 2), which corresponds to an increase in dust concentration.

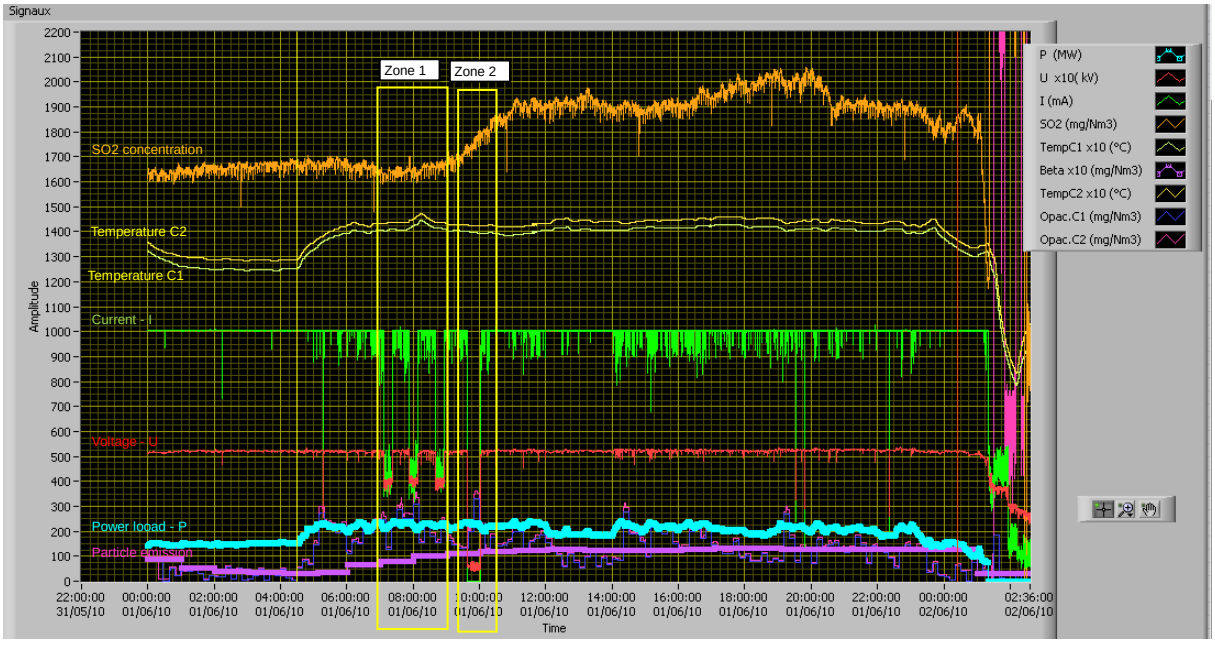

Figure 15 : Presentation of data from the unit and from the second field 2 of an operating ESP over a period of 26 hours.

3.2. Current-voltage measurement and their relation to the unit load

In order to highlight the influence of the load on electrical parameters, the voltage and the currents curves were plotted as function of the load (Figure 16).

Before looking in detail at each graph, it is apparent that the voltage and the current have upper limit values. The maximum current value is set by the power supply (1000 mA on all fields except field 121 which is 950 mA). The maximum voltage value, at the maximum power supply current, is linked to the dust content in the field; this, with other parameters defines the breakdown voltage.

On increasing the power of the unit, the maximum voltage in the first fields decreases as a function of the charge (Figure 16). This is linked to the flow of the flue gases which is greater at high power, which means that a shorter residence time is spent in the field and so the space charge level is higher at full power. This data shows that the voltage level in the two casings is not the same: this could be linked to different flow rates.

For the second fields, they have a maximum voltage which is less than that of the first fields (less space charge) and the voltage does not vary as a function of the power of the unit except for power less than 140 MW (the variations in concentration linked to the residence time in the field are weaker).

In the third field, the maximum voltage is weaker than that of the second field (less space charge) and the voltage does not vary as a function of the power of the unit (the variations in concentration are negligible).

The curves also shows the presence of the half-cycle suppression; a group of points is close to the maximum voltage supplied and another group is much lower (in all the fields except 122 and 131). The suppression of half-cycles is linked to the presence of back corona.

Figure 16 : Variation in the voltage as a function of the power for different fields in a casing.

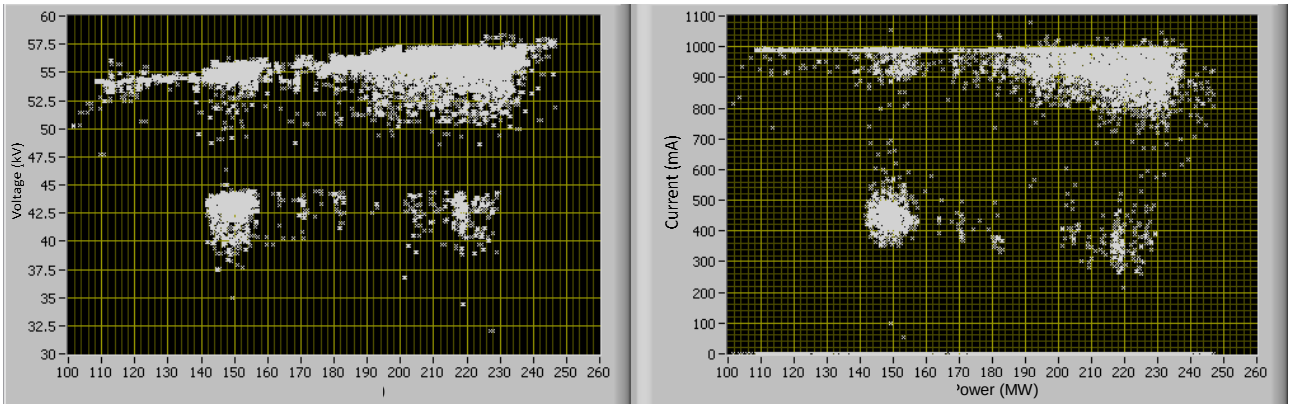

a – Field 1

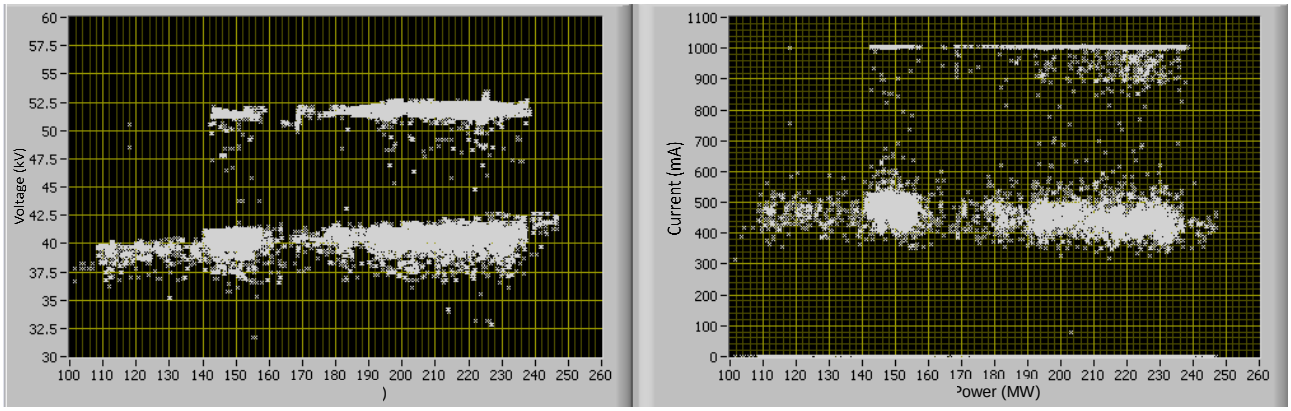

b – Field 2

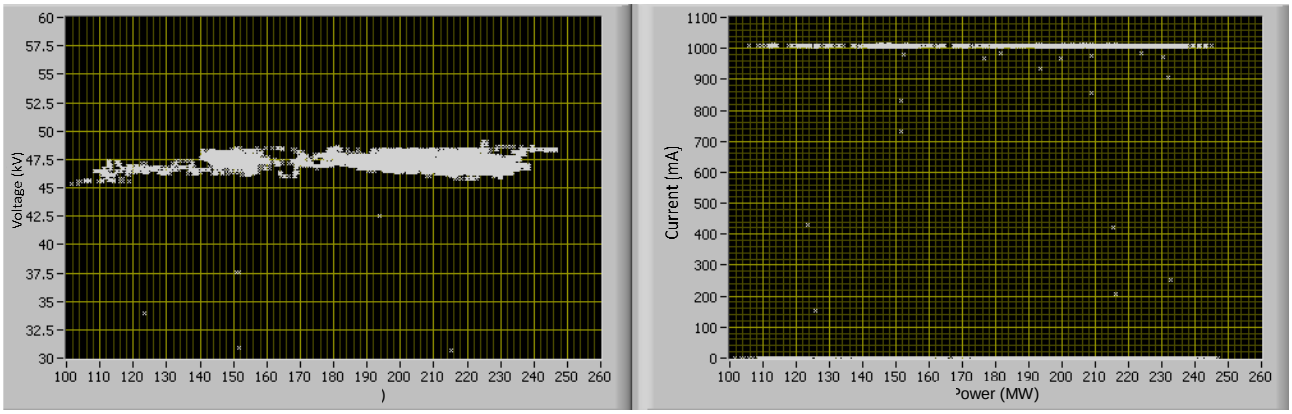

c – Field 3

3.3. Current-voltage curve characteristics

The suppression of half-cycles linked to the presence of back corona, as well as the control of the spark or the spark over provides the possibility to record a wide range of currents and voltages. In this case current voltage characteristics can be inferred and then used to detect faults in the electrostatic precipitator

The construction of voltage current characteristics can be divided in three phases:

- Initial treatment of the data recorded during one day
- Plot of the curves by quadratic regression on treated points
- Validation of the possibility to plot a characteristic current-voltage curve

The initial treatment of the data requires that:

1) periods of stable boiler load (when the power is approximately maximum) have to be identified and those when the power was reduced or inexistent have to be removed
2) the recorded currents and voltages have to be synchronized (the algorithmic data stockage employed did not allow for retrieval that would be in-phase with the other data from the unit).

The regression allows the plot of voltage current characteristics.

The validation of the characteristic current-voltage curve involves:

a) an evaluation of the reliability factor for the curve regression, (the coefficient has to be over 60%)
b) a check must be made that the threshold voltage is coherent with the channel width and lies between 10 and 40 kV.

Equipped with these precisions, the V-I curve can be constructed over a day timescale (provided that half-cycles have been suppressed or that there is enough recorded voltage variations).

An example of a quadratic regression using data from a day's operation is given in Figure 17.

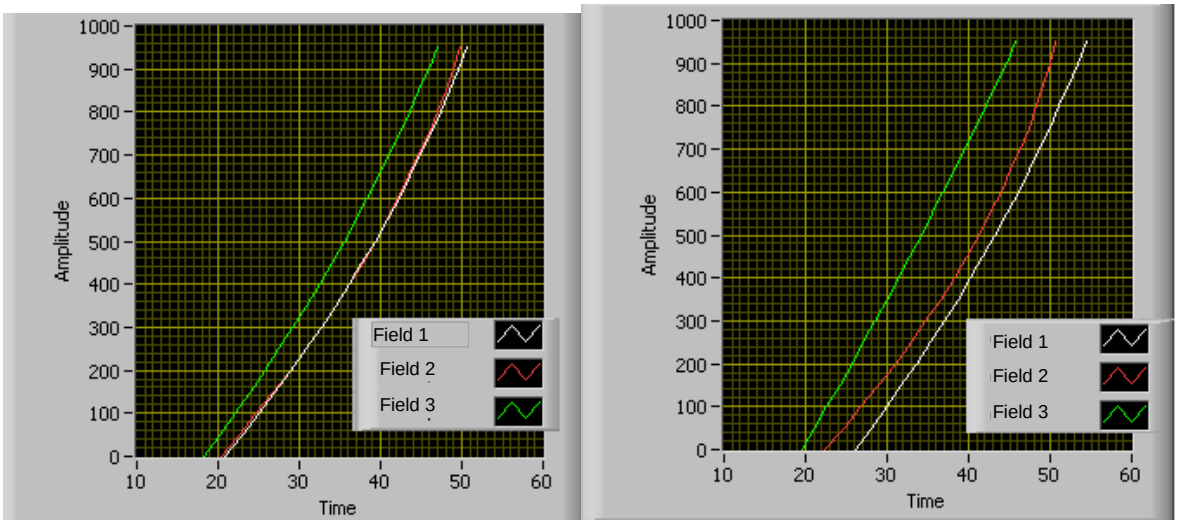

Figure 17: Reconstruction of the V-I curves from the two casings of the electrostatic filter

The space charge effect, associated with the dust particle concentration in each field, explains the voltage-current curve's displacement towards the right (more voltage for the same current level). The classic example is the order of the curves that lies between field 1 and field 3. The expected effect of the charged space is visible, and the order of the field is, in general, respected in casing 1.

It is also possible to consider analyzing the curves in order to enumerate the ESP's faults according to the algorithms defined in the reference [21].

3.4. Conclusion

Data recorded on the dust collector using intermittent energization were analysed in order to detect process modification and faults in the electrostatic precipitator. The ESP's performance can be evaluated as a function of process parameters or power supply status.

Current voltage characteristics can be inferred and then used to detect faults in the electrostatic precipitator. This is achieved without having to stop the installation and without having recourse to manual readings.

4. Perspectives

The presented studies show two different points of view concerning intermittent energization: the voltage - current data interpretation using low frequency collected unit data and the physical modelling.

Even if at first sight the recorded electrical data seems insufficient (due to a high monitoring period, less than one point every second), their treatment over an extended time scale reveals particular characteristics including faults in ESP.

Concerning modelling, the simulation of voltage from an applied current waveform, with or without intermittent energization, can be performed using a simplified ESP equivalent electric circuit. Accordingly, the efficiency of an ESP can be demonstrated using different means of regulation (with or without half-cycle suppression).

Further studies using this modelling could be also carried out to:

- automatically interpret the measured data and detect ESP's faults.
- simulate the Switch Mode Power Supply intermittent mode in order to confirm the improved collection efficiency resulting from increased flexibility in controlling the applied current.

Reference

[1] V. REYES, Electrical operation of precipitators - p192-249- Applied Electrostatic Precipitation- Edited by K.R. Parker – Black Academic & Professional- 1992

[2] H.J. WHITE, Electrical Energization - p1997-237 – Industrial Electro-static Precipitation – ISESP - 1963

[3] K. PARKER Electrical Operation of Electrostatic Precipitators, IET Power and Energy Series 41, London 2003

[4] K. PARKER and N. PLAKS, Electrostatic Precipitator (ESP) Training Manual, United States Environmental Protection Agency, July 2004, EPA-600/R-04-072

[5] R.J. TRUCE, “Back Corona and its Effects on the Optimisation of Electrostatic Precipitator Energisation control”, Seventh International Clean Air Conference, August 24-28, 1981

[6] HALLDIN, CLAES,and al. "Particle flow field in a commercial design ESP during intermittent energization." Proceedings of the Int. Conf. on Electrostatic Precipitation. 1996.

[7] K. PORLE, On Back Corona in Precipitators and Suppressing it Using Different Energization Methods, 3° ICESP Conference, Abano Terme (Italy) 1987

[8] Hezhong Tiang, Zhiguang Hu, Guaping Yang, Development on Simulating Software of High Voltage Energization System For Electrostatic Precipitator, ICESP VII CONFERENCE PAPERS, Kyongju, Korea, September 20-25. 1998

[9] E. C, LANDHAM, Jr. S; OGLESBY., Intermittent Energization with High Fly Ash Resistivity, ICESP V Conference papers, Washington, DC USA , April 5-8, 1993

[10] N. TACHIBANA, Y. MATSUMOTO, Intermittent energization on electrostatic precipitators, Journal of Electrostatics, Volume 25, Issue 1, June 1990, Pages 55-73, ISSN 0304-3886.

[11] S. MASUDA, A. MIZUNO, “Initiation condition and mode of back-discharge”, Journal of Electrostatics 4, 1977-78

[12] G. BACCHIEGA, I. GALLIMBERTI, V. ARRONDEL, N. CARAMAN, M. HAMLIL, “Back-corona model for prediction of ESP efficiency and voltage-current characteristics”, X ICESP, Cairns – Australia, 2006.

[13] G. BACCHIEGA, I. GALLIMBERTI, V. ARRONDEL, P. RAIZER, J. LECOINTRE, M. HAMLIL, “Static and dynamic back-corona characteristics”, IX ICESP, Kruger – South-Africa, 2004.

[14] V. ARRONDEL, J. SALVI, I. GALLIMBERTI, G. BACCHIEGA, “ORCHIDEE: Efficiency Optimisation of Coal Ash Collection in Electrostatic Precipitators”, IX ICESP, Kruger – South-Africa, 2004.

[15] B. BELLAGAMBA, F. MATTACHINI, I. GALLIMBERTI, R. TURRI, A. GAZZANI, U. TROMBONI, "A Mathematical Model for Simulation of Large Scale Electrostatic Precipitators", 5th International Conference on Electrostatic Precipitation, Washington D.C., 1993.

[16] I. GALLIMBERTI, A. GAZZANI, U. TROMBONI, E. LAMI, F. MATTACHINI, G. TREBBI, "Physical simulation of the particle migration in ESP, Part I - Model description", VI ICESP*, Budapest, 1996.

[17] I. GALLIMBERTI, A. GAZZANI, U. TROMBONI, E. LAMI, F. MATTACHINI, G. TREBBI, "Physical simulation of the particle migration in ESP, Part II - Application results", VI ICESP*, Budapest, 1996.

[18] I. GALLIMBERTI: "Recent advancements in the physical modelling of electrostatic precipitators", Journal of Electrostatics 43 (1998) 219-247, 1998.

[19] E. LAMI, F. MATTACHINI, I. GALLIMBERTI, R. TURRI, U. TROMBONI, "A Numerical Procedure for Computing the Voltage-Current Characteristics in ESP Configuration", Journal of Electrostatics 34 (1995) 385-399, 1994.

[20] I. GALLIMBERTI: “The Simulation of Corona Discharges Under Practical Precipitator Conditions, Symposium on the Transfer and Utilisation of Particulate Control technology“, EPRI-New Orleans, Vol. 1, November 1986

[21] V. ARRONDEL, G. BACCHIEGA, M. HAMLIL, N. GAUTIER, A. RENARD. “The crystal ball gazing with electrostatic precipitators: V-I curves analysis”, X ICESP, Hangzhou 2008